

Mercury–Mercury Tunneling Junctions. 1. Electron Tunneling Across Symmetric and Asymmetric Alkanethiolate Bilayers

Krzysztof Slowinski, Harold K. Y. Fong, and Marcin Majda*

Contribution from the Department of Chemistry, University of California at Berkeley, Berkeley, California 94720-1460

Received May 13, 1999

Abstract: Electron tunneling experiments involving Hg–Hg junctions incorporating two alkanethiolate monolayers are described. Formation of a symmetric junction (Hg–SC_n–C_nS–Hg) is accomplished by bringing in contact two small (3 × 10⁻³ cm²) mercury drop electrodes in a 5–20% (v/v) hexadecane solution of an alkanethiol. Formation of asymmetric junctions (Hg–SC_n–C_mS–Hg) and junctions containing *n*-alkane-3-thiopropanamide bilayers are also described. Tunneling currents in the junctions were measured for voltage biases extending to ±1.5 V. The currents decrease exponentially with the junction thickness yielding the tunneling decay constant, β = 0.89 ± 0.1 per CH₂. The decay constant exhibits only a weak dependence on the voltage bias suggesting that electron tunneling follows a through-bond mechanism. Tunneling currents in the *n*-alkane-3-thiopropanamide bilayer junctions were larger than those in alkanethiolate junctions with the same number of atoms suggesting that introduction of an amide group increases the strength of the electronic coupling through these types of σ-bonded systems.

Introduction

Electrochemical measurements of the long-range electron-transfer kinetics have contributed an increasing volume of new information to our understanding of electron tunneling phenomena.^{1,2} In this report, we describe formation of Hg–Hg tunneling junctions incorporating alkanethiolate-type monolayer films. The results reported below convince us that the mercury junction technique will further expand the range of experimental capabilities in this area.

Detailed electrochemical characterization of the distance and medium effects on the strength of electronic coupling have been successfully carried out for a number of molecular systems.^{3–7} Recent measurements involving alkanethiol monolayers, their derivatives, and strongly π-conjugated monolayer films have been particularly revealing.^{8–20} In this research, monolayer films

on electrodes play the dual role of the tunneling medium and a barrier structure designed to restrict access of a redox probe to the electrode surface to within a specific distance. A number of factors related to the structure of the metal electrodes and the chemical characteristics of the monolayer-forming molecules restrict the range of molecular systems that can be successfully used to play these two roles simultaneously.¹ Recent experiments with mercury electrodes showed that the liquid nature of this metal lends itself very well to the task of forming pinhole-free alkanethiolate-type monolayer films.^{21–25} Moreover, we have demonstrated recently that tunneling experiments combined with gradual expansion of the alkanethiolate-coated mercury drop electrodes can result in quantitative characterization of the strength of electronic coupling in alkanethiolate films along two pathways involving through-bond and chain-to-chain coupling.^{16,26} The Hg–Hg junctions and the tunneling experiments

* E-mail address: majda@socrates.berkeley.edu.

- (1) Finklea, H. O. *Electrochemistry of Organized Monolayers of Thiols and Related Molecules on Electrodes*. In *Electroanalytical Chemistry*; Bard, A. J., Rubinstein, I., Eds.; Marcel Dekker: New York, 1996; pp 109–335.
- (2) Miller, C. J. *Heterogeneous Electron-Transfer Kinetics at Metallic Electrodes*. In *Physical Electrochemistry: Principles, Methods, and Applications*; Rubinstein, I., Ed.; M. Dekker: New York, 1995; pp 27–79.
- (3) Li, T. T.-T.; Weaver, M. J. *J. Am. Chem. Soc.* **1984**, *106*, 6107.
- (4) Lipkowski, J.; Buess-Herman, C.; Lambert, J. P.; Gierst, L. J. *Electroanal. Chem.* **1986**, *202*, 169.
- (5) Chidsey, C. E. D. *Science* **1991**, *251*, 919.
- (6) Miller, C.; Cuendet, C. P.; Gratzel, M. J. *Phys. Chem.* **1991**, *95*, 877.
- (7) Forster, R. J.; Faulkner, L. R. *J. Am. Chem. Soc.* **1994**, *116*, 5444.
- (8) Finklea, H. O.; Hanshew, D. D. *J. Am. Chem. Soc.* **1992**, *114*, 3173.
- (9) Finklea, H. O.; Liu, L.; Ravenscroft, M. S.; Punturi, S. J. *Phys. Chem.* **1996**, *100*, 18852.
- (10) Becka, A. M.; Miller, C. J. *J. Phys. Chem.* **1992**, *96*, 2657.
- (11) Smalley, J. F.; Feldberg, S. W.; Chidsey, C. E. D.; Linford, M. R.; Newton, M. D.; Liu, Y.-P. *J. Phys. Chem.* **1995**, *99*, 13141.
- (12) Guo, L.-H. F.; McLendon, G. J. *Phys. Chem.* **1995**, *99*, 8458.
- (13) Gu, Y.; Waldeck, D. H. *J. Phys. Chem.* **1996**, *100*, 9573.
- (14) Cheng, J.; Saghi-Szabo, G.; Tossell, J. A.; Miller, C. J. *J. Am. Chem. Soc.* **1996**, *118*, 680.
- (15) Slowinski, K.; Chamberlain, R. V.; Bilewicz, R.; Majda, M. *J. Am. Chem. Soc.* **1996**, *118*, 4709.

- (16) Slowinski, K.; Chamberlain, R. V.; Miller, C. J.; Majda, M. *J. Am. Chem. Soc.* **1997**, *119*, 11910.
- (17) Yu, H. Z.; Shao, H. B.; Luo, Y.; Zhang, H. L.; Liu, Z. F. *Langmuir* **1997**, *13*, 5774.
- (18) Sachs, S. B.; Dudek, S. P.; Hsung, R. P.; Sita, L. R.; Smalley, J. F.; Newton, M. D.; Feldberg, S. W.; Chidsey, C. E. D. *J. Am. Chem. Soc.* **1997**, *119*, 10563.
- (19) Weber, K.; Hockett, L.; Creager, S. J. *Phys. Chem. B* **1997**, *101*, 8286.
- (20) Creager, S.; Yu, C. J.; Bamdad, C.; O'Connor, S.; MacLean, T.; Lam, E.; Chong, Y.; Olsen, G. T.; Luo, J.; Gozin, M.; Kayyem, J. F. *J. Am. Chem. Soc.* **1999**, *121*, 1059.
- (21) Demoz, A.; Harrison, D. J. *Langmuir* **1993**, *9*, 1046.
- (22) Bruckner-Lea, C.; Janata, J.; Conroy, J.; Pungor, A.; Caldwell, K. *Langmuir* **1993**, *9*, 3612.
- (23) Bruckner-Lea, C.; Kimmel, R. J.; Janata, J.; Conroy, J. F. T.; Caldwell, K. *Electrochim. Acta* **1995**, *40*, 2897.
- (24) Muskal, N.; Turyan, J.; Mandler, D. *J. Electroanal. Chem.* **1996**, *409*, 131.
- (25) Magnussen, O. M.; Ocko, B. M.; Deutsch, M.; Regan, M. J.; Pershan, P. S.; Abernathy, D.; Gruebel, G.; Legrand, J.-F. *Nature* **1996**, *384*, 250.
- (26) Slowinski, K.; Slowinska, K. U.; Majda, M. *J. Phys. Chem. B* 1999 in press.

described below further expand the range of our capabilities in the investigations of the electron tunneling kinetics.

Mercury has been used before in the formation of tunneling junctions. Mann and Kuhn used mercury to form various metal–LB–metal tunneling junctions (LB represents a Langmuir–Blodgett monolayer of variable chain length).²⁷ LB and self-assembled monolayer-type tunneling junctions (usually constructed by direct metal vapor deposition) and their properties have been a subject of several reports^{28,29} and reviews.^{30–32} Of most direct relevance to our research is a report of Porter and Zinn, who studied water structure in the Hg–Hg tunneling junctions.³³ They described electron tunneling experiments involving two Hg drop electrodes suspended at the adjacent 76 μm Pt disk electrodes. The Hg drops were progressively grown via mercury electrodeposition. While each of these experiments ended by coalescence of the two Hg drops, distinct levels of the tunneling current could be observed during the final stages of their growth. The tunneling current corresponded to just a few, ordered, molecular layers of water trapped between the mercury surfaces. In a more recent report, Rampi and co-workers described a method to form noncoalescing Hg–Hg junctions by bringing together two volumes of mercury in a glass tube (2.5 mm in diameter) filled with a solution of an alkanethiol. The junction capacitance was inversely proportional to the length of the alkanethiol chains (with $\epsilon = 2.7 \pm 0.3$) indicating that the junctions consist of two alkanethiolate monolayers.³⁴ The authors did not measure tunneling currents, due to the instability of the junctions at voltage biases in excess of 0.15 V.

Our Hg–Hg tunneling junction experiments involved two micrometrically driven hanging mercury drop electrodes (HMDE) described previously.¹⁶ Each Hg drop electrode was coated with an alkanethiolate monolayer via self-assembly.¹⁶ Subsequently, they were brought in contact using a micrometric positioning device to form a junction either in a solvent or in air. We show the exponential dependence of the observed tunneling currents on the number of carbon atoms in both symmetric and asymmetric junctions as well as in the case of bilayer junctions involving *n*-alkane-3-thiopropionamides. We also demonstrate that the tunneling decay constant β exhibits only a weak dependence on the voltage bias, indicating a through-bond tunneling mechanism, and discuss the advantages of the Hg–Hg tunneling junction method.

Experimental Section

Reagents. Fresh samples of the alkanethiols, C_nSH , $n = 10, 12, 14$, were purchased from TCI America (95+%); nonanethiol (95%) was purchased from Aldrich. They were used as received. The *n*-decane and *n*-dodecane derivatives of 3-thiopropionamide were synthesized by a one-step coupling of 3-thiopropionic acid with an appropriate primary amine.³⁵ A reaction mixture was refluxed overnight in THF in the presence of dicyclohexylcarbodiimide and 1-hydroxybenzotriazole. Following filtration, THF evaporation, and redissolution in chloroform,

(27) Mann, B.; Kuhn, H. *J. Appl. Phys.* **1971**, *42*, 4398.

(28) Polymeropoulos, E. E.; Sagiv, J. *J. Chem Phys.* **1978**, *1836*.

(29) Boulas, C.; Davidovits, J. V.; Rondelez, F.; Vouillaume, D. *Phys. Rev. Lett.* **1996**, *4797*.

(30) Ulman, A. *An Introduction to Ultrathin Organic Films; From Langmuir–Blodgett to Self-Assembly*; Academic Press: San Diego, 1991; Chapter 5.4, pp 367–384.

(31) Roth, S.; Burghard, M.; Fischer, C. M. Resonant Tunneling and Molecular Rectification in Langmuir–Blodgett Films. In *Molecular Electronics; IUPAC and Blackwell Science*; Jortner, J., Ratner, M., Eds.; Oxford, 1997; Chapter 8, pp 255–280.

(32) Petty, M. C. *Langmuir–Blodgett Films, An Introduction*; Cambridge University Press: New York, 1996; Chapter 6, pp 131–166.

(33) Porter, J. D.; Zinn, A. S. *J. Phys. Chem.* **1993**, *97*, 1190.

(34) Rampi, M. A.; Schueller O. J. A.; Whitesides, G. M. *Appl. Phys. Lett.* **1998**, *72*, 1781.

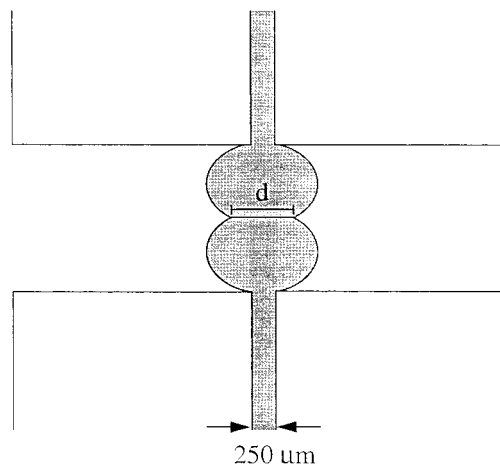


Figure 1. A schematic diagram showing the shape and the extent of deliberately induced distortion of two mercury drops forming a tunneling junction. The cross sectional diameter of the junction (d) is ca. 600 μm . The two mercury drops were formed at the tips of 250 μm glass capillaries as described in the Experimental Section. All the dimensions in the drawing are approximately to scale.

the amides were purified on a silica column with 60:40 CH_2Cl_2 :EtOAc mixture. This coupling procedure gave the products with a yield of 50–60%. The identity of the product was confirmed by elemental analysis and ^1H NMR spectroscopy. The later yielded spectra with the identical position of all resonances to those reported for the *n*-pentadecane derivative by Clegg and Hutchison.³⁶ Elemental analysis: Calcd for *n*-decane derivative ($\text{C}_{13}\text{H}_{27}\text{NOS}$): C, 63.62; H, 11.08; N, 5.71. Found: C, 62.2; H, 10.8; N, 5.2. Calcd for *n*-dodecane derivative ($\text{C}_{15}\text{H}_{31}\text{NOS}$): C, 65.88; H, 11.42; N, 5.12. Found: C, 63.0; H, 10.4; N, 4.4. Mercury (Quicksilver Products Inc., triply distilled) was used without further purification. The following reagents were also used as received: hexadecane (Aldrich, 99+% anhydrous), chloroform (Aldrich, reagent grade), ethanol and ethyl acetate (Fisher, reagent grade), methanol (Fisher, spectroscopic grade), and NaClO_4 (Fisher, purified grade). House-distilled water was passed through a four-cartridge Barnstead Nanopure II purification system. Its resistivity was in the range 17.6–18.3 $\text{M}\Omega\text{ cm}$.

Hg–Hg Tunneling Junctions. The mercury junctions were assembled using two micrometrically driven hanging mercury drop electrodes (HMDE). These were Kemula–Kublik-type³⁷ constructed using Guidelli's design³⁸ as described earlier.¹⁶ Silanized, 250 μm diameter capillaries were used. The two electrodes were positioned vertically and coaxially, one above the other, with the top electrode mounted on a vertically moveable stage. A small glass cell was mounted coaxially with the glass capillary of the bottom HMDE, allowing for immersion of a junction in a desired alkanethiol solution or pure solvent. Most experiments were done in 5–20% (v/v) hexadecane solutions of a selected alkanethiol. Thus the self-assembly of an alkanethiol monolayers took place momentarily upon generation of the new Hg drops ($A = 0.03\text{ cm}^2$).¹⁶ The junctions were always formed at open circuit. Formation of the junction was monitored visually with a stereomicroscope providing 20-fold magnification. Following the initial pointlike contact of the Hg drops, the junction area was increased to ca. $3 \times 10^{-3}\text{ cm}^2$ by a deliberate, further decrease of the gap between the tips of the two HMDE capillaries. This resulted in a small distortion of the two Hg drops as shown in Figure 1 (see also Results and Discussion). The junction area (A_j) was measured by visual assessment of the Hg–Hg contact length, d (of ca. 600 μm), relative to the known (250 μm) diameter of the two capillaries. We estimate that the precision

(35) Kiso, Y.; Yajima, H. Amide Formation, Deprotection, and Disulfide Formation in Peptide Synthesis. In *Peptides. Synthesis, Structures, and Applications*; Gutte, B., Ed.; Academic Press: San Diego, 1995; Chapter 2, pp 40–91.

(36) Clegg, R. S.; Hutchison, J. E. *Langmuir* **1996**, *12*, 5239.

(37) Kemula, W.; Kublik, Z. *Anal. Chim. Acta* **1958**, *18*, 104.

(38) Becucci, L.; Moncelli, M. R.; Guidelli, R. *J. Electroanal. Chem.* **1996**, *413*, 187–194.

of that step was ca. $\pm 100 \mu\text{m}$. This in turn resulted in ca. $\pm 30\%$ uncertainty (ΔA_j) in the determination of the junction's surface area ($\Delta A_j = 0.5\pi d \Delta d$). All current–voltage bias measurements were done with a BAS 100A electrochemical analyzer in a two-electrode configuration at room temperature of ca. 20°C . The measurements of the junction capacitance involved recording i – V curves in a 5–20% (v/v) hexadecane solution of an alkanethiol at 52 V/s extending to ± 50 mV around zero bias. We note that the use of more polar solvents in these measurements (particularly methanol and ethanol) resulted in substantially larger capacitance values. This is due to the presence of ionic impurities in these solvents and the resulting contribution to the measured capacitance from the mercury surfaces outside the junction. The values of the tunneling currents were corrected by subtraction of the capacitive component.

Results and Discussion

Two methods of the Hg–Hg junction formation procedure were established. (1) The junctions can be formed directly in a solution of an alkanethiol ($C_n\text{SH}$) as described in the Experimental Section. This procedure results in the formation of symmetric junctions (Hg– C_n – C_n –Hg) as in Rampi's experiments.³⁴ (2) To form asymmetric junctions (Hg– C_n – C_m –Hg), one electrode was coated with a monolayer of an alkanethiol ($C_n\text{SH}$) and then it was brought in contact with the second electrode in a solution of a different alkanethiol ($C_m\text{SH}$). Most tunneling data were collected in hexadecane. While we did not attempt to systematically screen many solvents, equally reliable results can also be obtained in ethyl acetate, acetone, and ethanol. Although less stable with time, both types of junctions can also be formed in the absence of a solvent (in the air). Reproducible current vs voltage bias (i – V) curves can be readily recorded with very small junctions formed upon the first, essentially point contact between the mercury drops. Nevertheless, to more precisely measure the junction area, we relied on larger junctions (ca. $3 \times 10^{-3} \text{ cm}^2$ in contact area), obtained by further decreasing the gap between the two capillary tips supporting the Hg drops (see Experimental Section). The final position and shape of the mercury drops is depicted schematically in Figure 1. It is interesting to note that in most cases of junction assembling (hundreds of individual experiments), we have observed a sudden, minuscule, but easily detectable “jump” or “twitch” of the two Hg drops. In some cases, a small jump takes place shortly after the initial contact of the Hg drops and results in a sudden increase of the junction contact to ca. 0.003 cm^2 . In other cases, a minute twitch of the contacting drops is observed seconds *after* the two Hg drops were slowly distorted and the final junction contact area was established. (An area of ca. 0.003 cm^2 was chosen in those cases precisely in an attempt to reproduce the junction size spontaneously assumed by the two drops in the “jump” events.) The twitch events result in no apparent change of the junction area. We associate these sudden jump/twitch events with squeezing of solvent from the junction powered by the van der Waals attraction forces acting on the two alkanethiolate-coated mercury surfaces.

Figure 2 shows two typical i – V traces obtained in two different experiments with Hg– C_{12} – C_{12} –Hg junctions. Trace A corresponds to a junction formed between a Hg drop electrode and a 1 cm^2 mercury pool electrode in a 5% $C_{12}\text{SH}$ hexadecane solution. A large hysteresis was always observed during the first i – V half-cycle. It is likely that this behavior reflects removal of the solvent initially trapped in the junction. Trace B corresponds to a junction formed between two Hg drop electrodes as described above. The i – V curves obtained with this type of junction were significantly more reproducible and rarely burdened with any hysteresis. Clearly, the use of two spherical Hg electrodes is a preferred strategy in the formation

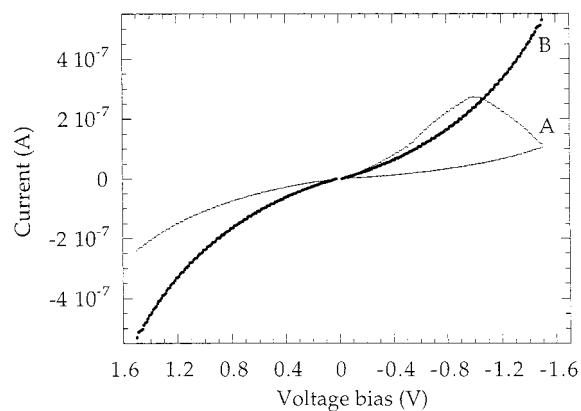


Figure 2. Two i – V curves obtained for Hg– C_{12} – C_{12} –Hg tunneling junctions in a 10% (v/v) hexadecane solution of dodecanethiol: (A) the junction was formed between an Hg drop electrode and a 1 cm^2 Hg pool; (B) the junction was formed between two Hg drop electrodes. In both cases, the junction area ($A_j = 3 \times 10^{-3} \text{ cm}^2$) is approximately the same.

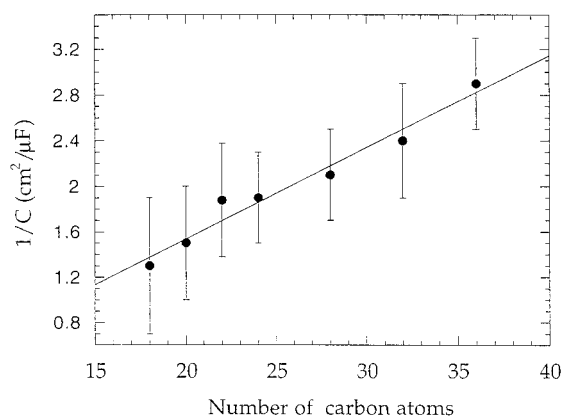


Figure 3. A plot of the inverse capacitance values vs the total number of carbon atoms in the symmetric alkanethiolate junctions. The data represent averages and standard deviations of 10 independent measurements for each type of junction.

of well-behaved mercury junctions. So far, we were unable to form junctions with shorter alkanethiolates than $C_9\text{SH}$. Once formed, the C_9 – C_9 junctions are stable for only ca. 1 min. Thicker junctions are progressively more stable. The highest voltage bias that can be applied across a junction without inducing mercury coalescence appears to depend on the alkane chain length. Although this property of the junctions has not been systematically investigated, the C_{16} – C_{16} bilayer junctions are stable under voltages as large as ± 2.5 V. Tunneling currents for all junctions reported below were measured at ± 1.5 V. Initial characterization of all the junctions involved measurements of their capacitance. A plot of $1/C$ vs n for n in the range 18–36 (n is a total number of alkane carbon atoms in the bilayer assembly) is shown in Figure 3. Linearity of that plot indicates that the junctions behave as ideal parallel plate capacitors. The slope yielded an average value of the dielectric constant $\epsilon = 2.0 \pm 0.3$, a value consistent with similar measurements by Rampi et al.³⁴ and other literature reports for alkanethiol monolayer films.^{6,15,39} The thicknesses of our junctions obtained from the measured capacitances using this ϵ value were in agreement with those calculated using a simple bilayer model. Specifically, the thickness calculations assumed known, perpendicular orientation of all-trans alkane chains with respect to

(39) Porter, M. D.; Bright, T. B.; Allara, D. L.; Chidsey, C. E. D. *J. Am. Chem. Soc.* **1987**, *109*, 3559.

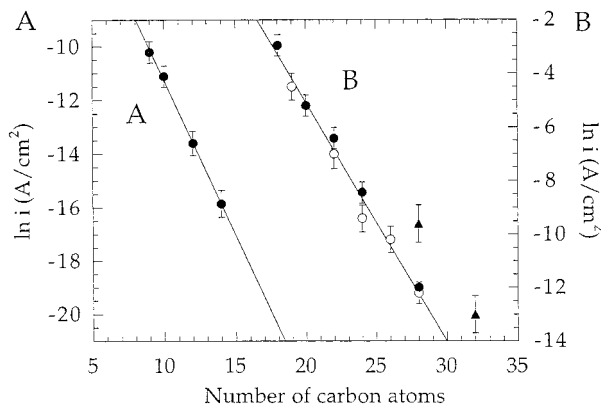


Figure 4. Plots of the logarithm of the tunneling currents obtained with (A) a single Hg drop electrode coated with different alkanethiolate monolayers recorded at an overpotential of -0.45 V in a 0.5 M KCl, 1.0 mM $\text{Ru}(\text{NH}_3)_6^{3+}$ solution (data from ref 16) and (B) Hg–Hg junctions formed with symmetric alkanethiolate bilayers of a given total number of carbon atoms (black circles), asymmetric alkanethiolate bilayers (Hg– C_n – C_m –Hg, total number of carbon atoms = $n + m$) with $n:m = 9:10, 10:12, 10:14, 12:14,$ and $12:16$ (open circles), and symmetric n -decane-3-thiopropylamide and n -dodecane-3-thiopropylamide for which “number of carbon atoms” includes the nitrogen atoms of the amide group (black triangles). Data in plot B were recorded in 5–20% (v/v) hexadecane solutions of the alkanethiols and represent averages and standard deviations of 10 measurements with newly assembled junctions obtained at a voltage bias of -1.5 V (see Figure 2B). The n -alkane-3-thiopropylamide monolayers were formed on Hg electrodes from their ethanol solutions and the junctions were then assembled and investigated in hexadecane.

the Hg surfaces²⁵ and no chain intercalation at the bilayer midplane, and relied on the known values of the bond lengths and angles.¹⁶ This agreement is reassuring, but in view of poor precision of the capacitance measurements (related to low precision of the junction area measurements), it does not eliminate a possibility of some chain disorder and/or their midplane intercalation. Independent, precise junction thickness measurements are required to resolve this and other structural issues.

In the measurements of the tunneling currents, the voltage bias was applied linearly with a scan rate ranging from 0.1 to 50 V/s. In the case of the thinnest junction, fast scan rates were used to eliminate a small hysteresis observed between the forward and reverse currents. In all other cases, the magnitude of the scan rate did not have any significant effect on the magnitude of the observed tunneling current. A priori, one could expect that the electrostatic force between two charged Hg surfaces ($F = \epsilon\epsilon_0 AV^2/2h^2$, where V is voltage bias and h is the thickness of the junction) might result in higher currents at larger biases due to the progressively larger distortion of the Hg drops increasing the surface area of the junction. One could also argue that a decreasing Hg surface tension with charging might enhance that process. However, these voltage-induced distortions of the mercury drops should be more pronounced at slow than at fast bias scan rates. The fact that the scan rate has no effect on the magnitude of the tunneling current (with an exception of a small hysteresis observed for C_9 – C_9 junctions) suggests that the distortions are negligible. We believe that the initial distortion of the Hg drops deliberately applied to increase the junction surface area eliminates or minimizes that effect.

The dependence of $\ln(i)$ on n is shown in Figure 4 for a number of symmetric and asymmetric junctions. The data were obtained at 1.5 V by averaging current values obtained in 10 independent measurements for each type of junction. The

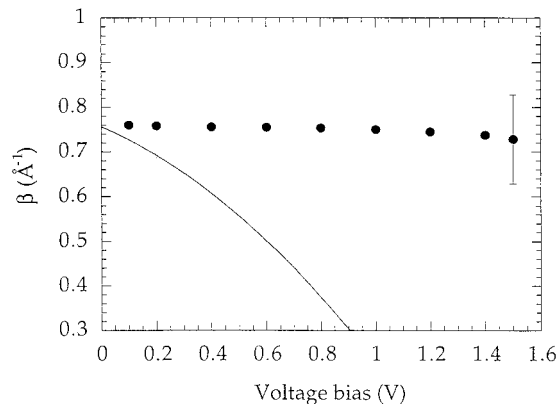


Figure 5. The dependence of the tunneling decay constant β on the voltage bias obtained for the symmetric Hg–Hg junctions with nonane-, decane-, and dodecanethiolate bilayers (black circles) and calculated according to Simmons theory⁴³ (continuous line; see discussion in the text). The data correspond to averages of 10 separate i – V curves recorded for each of the three junctions.

linearity of this dependence indicates that conduction across the junction involves electron tunneling.^{1,2,30,40} Although the decay constant, $\beta = 0.89 \pm 0.1$ per CH_2 , is somewhat smaller than the value $\beta = 1.14 \pm 0.09$ per CH_2 obtained in our experiments with alkanethiolate-coated Hg drop electrodes (also reproduced in Figure 4),¹⁶ it remains within a range of previously reported values.^{1,2} Also included in Figure 4 are two data points corresponding to junctions formed with n -decane- and n -dodecane-3-thiopropylamides ($\text{HS}-(\text{CH}_2)_2-\text{CONH}-(\text{CH}_2)_n-\text{H}$ with $n = 10$ or 12). Significantly higher values of the tunneling current obtained in these two cases, relative to the alkanethiolate junctions of the same number of atoms, indicate that insertion of an amide group results in an increase of the electronic coupling. In support of this observation, Clegg and Hutchison reported recently a substantially increased strength of electronic coupling across σ -bonded fragments with three consecutive amide groups.⁴¹ This effect could be related to the presence of the lateral hydrogen bonding between the amide groups. The latter was determined earlier by Clegg and co-workers on the basis of their external reflective FTIR spectroscopy data obtained with monolayers of the analogous compounds on gold.^{36,42} We note that the surface densities of these n -alkane-3-thiopropylamides on Hg are the same as those obtained for alkanethiols.¹⁶ To make this determination, we carried out coulometric experiments described previously to measure charge due to oxidative coupling of the n -alkane-3-thiopropylamides to Hg.¹⁶ Single Hg drop electrodes were used in ethanol/water (2:1) NaClO_4 electrolytes. These measurements yielded values corresponding to areas per molecule of $20.5 \text{ \AA}^2/\text{molecule}$. This is an identical value to that we reported for alkanethiols¹⁶ and consistent with the coverage assessment by Clegg et al.³⁶ This shows that the presence of the amide groups does not lead to a looser packing density. Consequently, the higher tunneling currents reported here cannot be explained by postulating a partial collapse or a substantial intercalation of the terminal alkane chains in the bilayer junctions formed with the two n -alkane-3-thiopropylamides.

In Figure 5, we compare the experimentally determined dependence of β on V with the Simmons theory of electron

(40) Barbara, P. F.; Meyer, T. J.; Ratner, M. A. *J. Phys. Chem.* **1996**, *100*, 13248.

(41) Clegg, R. C.; Hutchison, J. E. Meeting Abstracts, Vol. 99-1, No. 919, The Electrochemical Society, Inc., 1999.

(42) Clegg, R. S.; Reed, S. M.; Hutchison, J. E. *J. Am. Chem. Soc.* **1998**, *120*, 2486.

tunneling between two metal plates across a dielectric layer through a square potential energy barrier, ϕ .⁴³ This theory yields $\beta = (4\pi/h)[2m(\phi - V/2)]^{1/2}$, where m is the mass of electron. Clearly, electron tunneling in our junctions involving alkanethiolate bilayers does not conform to this square barrier model. The weak dependence of β on V observed here and also reported by others in electrochemical experiments with monolayer-coated electrodes^{10,13,44} appears to be a signature of the through-bond mode of electron tunneling.

Concluding, the Hg–Hg junctions described here present several important advantages in the studies of electron tunneling processes relative to the usual electrochemical methods. (1) Since electron tunneling does not involve a redox probe, the junction method can tolerate some density of pinhole defects. Similarly, background processes such as mercury electrooxidation and monolayer desorption do not affect tunneling current measurements in the junction method. For example, due to background processes, monolayers formed with *n*-alkane-3-thiopropionamides mentioned above are not sufficiently stable on Hg drop electrodes in the aqueous electrochemical experiments with redox probes. However, they could be successfully investigated with the Hg–Hg junction method. (2) The junction experiments result intrinsically in significantly higher currents since electron tunneling takes place between two metal electrodes representing much larger densities of electronic states than those typically encountered for solutions of redox species (see Figure 4). Moreover, the junction experiments can be carried out over a wider range of voltages. This allows one to extend electron tunneling investigations to significantly thicker

(43) Simmons, J. G. *J. Appl. Phys.* **1963**, 34, 1793.

(44) Xu, J.; Li, H.-L.; Zhang, Y. *J. Phys. Chem.* **1993**, 97, 11497.

molecular films compared to the electrochemical experiments. In the latter case, background processes, inability to exponentially increase rates of electron transfer beyond overpotentials in excess of reorganization energy, as well as possible mass transport limitations, restrict the thickness of molecular films that can be studied electrochemically to ca. 18–20 σ -bonds. (3) Well-behaved character of the mercury junctions stemming from the atomically smooth surfaces of liquid mercury allows us to project that this methodology can be extended to microscopic junctions using significantly smaller Hg drops suspended on Pt microdisk electrodes. With microscopic junctions, investigations of single-electron tunneling phenomena would contribute to the rapidly growing field of molecular electronics.^{45, 46}

Acknowledgment is made to the donors of the Petroleum Research Fund, administered by the American Chemical Society, for partial support of this research. Additional support was provided by a grant from the National Science Foundation CHE-942269. Synthesis of the *n*-alkane-3-thiopropionamides was carried out by K. Slowinska (UCB), J. C. Fong (UCB), and Dr. H. Van Ryswyk (Harvey Mudd College) as a collaborative project supported in part by a Summer Research Fellowship supplement from The Petroleum Research Fund. We are grateful for their contribution to this project.

JA991613I

(45) Grabert, H.; Devoret, M. H. *Single Charge Tunneling, Coulomb Blockade Phenomena in Nanostructures*; Grabert, H., Devoret, M. H., Eds.; Plenum Press: New York, 1992.

(46) *Molecular Electronics*; Jortner, J., Ratner, M., Eds.; IUPAC and Blackwell Science: Oxford, 1997.